Sensitivity to Voltage-Independent Inhibition Determined by Pore-Lining Region of the Acetylcholine Receptor

Michael M. Francis,*# Kyung Il Choi,§ Benjamin A. Horenstein,§ and Roger L. Papke*#
Departments of Neuroscience,* Pharmacology and Therapeutics,# and Chemistry,§ University of Florida, Gainesville, Florida 32610 USA

ABSTRACT Some noncompetitive inhibitors (e.g., ganglionic blockers) exhibit selectivity for the inhibition of neuronal nicotinic acetylcholine receptors (nAChRs). This study characterizes the mechanism of selective long-term inhibition of neuronal and muscle-neuronal chimeric nAChRs by bis(2,2,6,6-tetramethyl-4-piperidinyl) sebacate (bis-TMP-10 or BTMPS), a bifunctional form of the potent ganglionic blocker tetramethylpiperidine. Long-term inhibition of neuronal nAChRs by bis-TMP-10 has been previously demonstrated to arise, at least in part, from the binding of the bis compound to neuronal β-subunits. In this study, long-term inhibition is demonstrated to be dependent upon the presence of sequence element(s) within the pore-lining second transmembrane domain (tm2) of neuronal β-subunits; however, the inhibitor binding site itself does not appear to be contained within the segment of the channel pore influenced by the membrane electric field. Specifically, our results imply that bis-TMP-10 interacts with an activation-sensitive element, the availability of which may be regulated by a sequence in the tm2 domain. Furthermore, we demonstrate a compound length requirement for long-term inhibition that would be consistent with binding to multiple sites located on the extracellular portion of the receptor.

INTRODUCTION

Neuronal nicotinic acetylcholine receptors (nAChRs) are pentameric complexes (Anand et al., 1991, Cooper et al., 1991) and share a considerable number of structural and functional features with muscle-type nAChRs. Structural similarities of individual subunits include a large amino-terminal extracellular domain followed by four putative transmembrane segments with a large intracellular domain between transmembrane domains three and four (for review, see Changeux et al., 1992; Karlin and Akabas, 1995). Whereas muscle-type nAChRs are composed of four distinct proteins (α1, β1, γ or ϵ, and δ in the ratio of 2:1:1:1), functional neuronal nAChRs can be composed of as few as two (α-β heteromers) or, in some cases, one class of subunit (α-subunit homomers). Eight different genes encoding putative neuronal α-subunits (α2–α9) and three different genes (β2–β4) coding for putative β-subunits have been cloned to date. Pairwise injection of the neuronal α-subunit genes α2, α3, α4, and, in some instances, α6 with the β-subunit genes β2 or β4 provides for the expression of receptors with pharmacologically and physiologically distinct activation profiles in *Xenopus* oocytes (Gerzanich et al., 1997; Luetje and Patrick, 1991). This situation both simplifies the study of heterologously expressed receptor subtypes and complicates efforts to assign specific functional correlations between heterologously expressed receptor subtypes and the receptor subtypes expressed in vivo. Studies examining the subunit composition of peripheral or ganglionic neuronal nAChRs have shown that receptors may include the α3, α5, β4, and/or β2 subunits (Conroy and Berg, 1995). It has been demonstrated that inclusion or exclusion of particular subunits will confer particular functional roles and pharmacological sensitivities on nAChRs (for review, see Papke, 1993; Sargent, 1993). In keeping with this idea, certain classes of noncompetitive inhibitors known as ganglionic blockers show selectivity for the inhibition of neuronal nAChRs.

The ganglion blocking activity of two such compounds, 2,2,6,6-tetramethylpiperidine (TMP) and 1,2,2,6,6-pentamethylpiperidine or pempidine (PMP), has been well documented in the literature (Lee et al., 1958; Spinks and Young, 1958). More recently, it was reported that neuronal nAChRs exhibit more prolonged inhibition in response to co-application of ACh with a bifunctional analog of TMP, bis(2,2,6,6-tetramethyl-4-piperidinyl sebacate (bis-TMP-10 or BTMPS), whereas muscle-type nAChRs recover completely from inhibition within 5 min (Papke et al., 1994). Furthermore, inhibition of neuronal nAChRs by bis-TMP-10 was demonstrated to be use dependent and have an approximate IC50 of 200 nM under experimental conditions of high p_{open}. In addition, the time course of recovery from inhibition was shown to be dependent on both the class of β-subunit present (β1 or β4/β2) and, for the $\alpha\beta\delta$ and $\alpha\beta\gamma$ subunit combinations, the presence or absence of the δ-subunit (Francis and Papke, 1996; Papke et al., 1994). Bis-TMP-10 is a member of the bis-TMP-*n* series of compounds, which share a common structure consisting of a symmetrical diester of methylated piperidinol rings linked by an aliphatic diacid chain containing *n* carbons. Because of the bifunctional nature of bis-TMP-10, it was hypothe-

Received for publication 5 September 1997 and in final form 4 February 1998.

Dr. Choi's current address: Division of Applied Science, Korea Institute of Science and Technology, P.O. Box 131, Cheongryang, Seoul 130–650, Korea.

Address reprint requests to Dr. Roger L. Papke, Department of Pharmacology and Therapeutics, University of Florida, Gainesville, Florida 32610-0267. Tel.: 352-392-4712; Fax: 352-392-9696; E-mail: rpapke@college.med.ufl.edu.

0006-3495/98/05/2306/12 $2.00

sized that long-term inhibition arises as a result of the potential for binding of the piperidinol rings to distinct sites.

In the case of muscle-type nAChRs, a number of investigators have used noncompetitive inhibitors in conjunction with site-directed mutagenesis or photoaffinity labeling as probes for structure. These studies have localized the binding of noncompetitive blockers of muscle-type nAChRs to the putative pore-lining second transmembrane domain (tm2) or the short extracellular loop (ecl) region between tm2 and transmembrane domain 3 (Charnet et al., 1990; DiPaola et al., 1990; Giraudat et al., 1986; Giraudat et al., 1987; Leonard et al., 1988; Pedersen et al., 1992; White and Cohen, 1992). Recently, more detailed insights regarding structure-function relationships have been obtained either by examination of the accessibility of substituted cysteines to covalent modification or by examination of the functional effects of unnatural amino acid incorporation (Akabas et al., 1992, 1994; Kearney et al., 1996).

The experiments described in the present study seek to extend the analysis of structure-function relationships to neuronal nAChRs by examining subunit-specific determinants of sensitivity to use-dependent inhibition. To characterize the mechanism for the selective long-term inhibition of neuronal nAChRs, we have created a pair of chimeric β-subunits that exchange eight amino acids of tm2 between muscle (β1) and neuronal β-subunits (β4 in this case) and a third chimeric β-subunit in which eight amino acids of the β4 subunit ecl region is replaced with the homologous sequence from β1.

Long-term inhibition of neuronal nAChRs by bis-TMP-10 is shown to be dependent upon the β-subunit tm2 region, although apparently independent of binding to elements of tm2 located within the membrane electric field or accessible to open-channel blockers. Because the inhibition is use dependent, this observation implies binding to sites for which availability depends both upon channel opening and interactions with specific sequence elements in tm2. These findings highlight the dynamic nature of channel gating and emphasize the importance of interactions between tm2 and surrounding structural elements with channel activation.

MATERIALS AND METHODS

Chemicals and synthesis

Fresh acetylcholine (Sigma Chemical Co., St. Louis, MO) stock solutions were made daily in Ringer's solution and diluted. Bis-TMP-10 was obtained from Ciba-Geigy (Hawthorne, NY), and TMP was obtained from Aldrich Chemical Co. (Milwaukee, WI). Bis(2,2,6,6,-tetramethyl-4-piperidinyl) succinate (bis-TMP-4) was synthesized by Ciba-Geigy and obtained from Dr. H. Glossmann (Glossmann et al., 1993). All other chemicals for electrophysiology were purchased from Sigma. Chemicals used for the synthesis were purchased from Aldrich. A general synthetic procedure and the characterization of the synthesized compounds are described below.

General synthetic procedure

To a mixture of 2,2,6,6-tetramethyl-4-piperidinol (3.0 mmol) and one equivalent of the corresponding ester, unless otherwise specified, in 2 ml of dimethyl formamide was added 250 mg of powdered potassium carbonate. The resulting mixture was heated at 145–150°C for 24–72 h under a gentle stream of N_2. After cooling, the reaction mixture was partitioned between water and methylene chloride. The organic layer was separated, washed with water and brine, dried (anhydrous $MgSO_4$), and evaporated to dryness to give a crude product, which was purified via salt formation (HCl or acetic acid), extraction, or column chromatography. All compounds were recrystallized before use in electrophysiology experiments.

*Bis-TMP-*n *compounds*

These compounds are inhibitors that differ from bis-TMP-10 only in the length of the aliphatic chain, where *n* stands for the total number of carbons in the diester linker. Structures are shown in Fig. 6.

Bis(2,2,6,6-tetramethyl-4-piperidinyl) hexanedioate (bis-TMP-6)

The title compound was synthesized from dimethyl adipate in 38% yield, recrystallized from hexane, and then precipitated from hexane as the acetate salt with a melting point of 135–140°C. ^{1}H NMR (300 MHz, D_2O, δ): 1.47 (12H, s), 1.51 (12H, s), 1.63 (4H, m), 1.73 (4H, dd, J_1 = 10.6 Hz, J_2 = 13.6 Hz), 1.90 (4.5H, s), 2.16 (4H, dd, J_1 = 4.1 Hz, J_2 = 14.0 Hz), 2.42 (4H, m), 5.28 (2H, m). ^{13}C NMR (D_2O, δ): 22.65, 23.84, 25.47, 29.26, 33.84, 39.39, 57.55, 66.13, 175.57, 179.89. LRMS (ESI) 425.3, MH^+.

Bis(2,2,6,6-tetramethyl-4-piperidinyl) octanedioate (bis-TMP-8)

The title compound was synthesized from dimethyl octanedioate in 72% yield and was recrystallized from *n*-pentane. Melting point was 90°C. ^{1}H NMR (300 MHz, $CDCl_3$, δ): 1.14 (4H, t, J = 11.7 Hz), 1.16 (12H, s), 1.24 (12H, s), 1.36 (4H, m), 1.91 (4H, dd, J_1 = 12.6 Hz, J_2 = 4.1 Hz), 2.28 (4H, t, J = 7.4 Hz), 5.19 (2H, tt, J_1 = 11.7 Hz, J_2 = 4.1 Hz); ^{13}C NMR ($CDCl_3$, δ): 24.77, 28.71, 28.97, 34.54, 34.80, 43.92, 51.40, 68.52, 173.15; HRMS (FAB, MH^+): calculated for $C_{26}H_{49}N_2O_4$ 453.3692, found 453.3691.

Bis(2,2,6,6-tetramethyl-4-piperidinyl) dodecanedioate (bis-TMP-12)

The title compound was synthesized from dimethyl dodecanedioate, which was prepared from dodecanedioic acid and methanol by using thionyl chloride in 77% yield and was recrystallized from *n*-pentane. Melting point was 75–76°C. ^{1}H NMR ($CDCl_3$, δ): 1.14 (4H, t, J = 11.7 Hz), 1.15 (12H, s), 1.24 (12H, s), 1.28 (12H, brs), 1.61 (4H, m), 1.91 (4H, dd, J_1 = 12.6 Hz, J_2 = 4.1 Hz), 2.27 (4H, t, J = 7.4 Hz), 5.19 (2H, tt, J_1 = 11.7 Hz, J_2 = 4.1 Hz); ^{13}C NMR ($CDCl_3$, δ): 24.94, 29.00, 29.04, 29.18, 29.32, 34.63, 34.79, 43.93, 51.37, 68.45, 173.26; HRMS (FAB, MH^+): calculated for $C_{30}H_{57}N_2O_4$ 509.4318, found 509.4329.

Preparation of RNA and expression in *Xenopus* oocytes

The preparation of in vitro synthesized cRNA transcripts and oocyte injection have been described previously (Boulter et al., 1987). Briefly, in vitro cRNA transcripts were prepared using the appropriate mMessage mMachine kit from Ambion (Austin, TX) after linearization and purification of cloned cDNAs. Two to three ovarian lobes were surgically removed and then cut open to expose the oocytes. The ovarian tissue was then treated with collagenase from Worthington Biochemical Corp. (Freehold, NJ) for 2 h at room temperature (in calcium-free Barth's solution: 88 mM NaCl, 10 mM HEPES, pH 7.6, 0.33 mM $MgSO_4$, 0.1 mg/ml gentamicin sulfate). Subsequently, stage 5 oocytes were isolated and injected with 50 nl each of a mixture of the appropriate subunit cRNAs after harvest.

Recordings were made 2–7 days after injection depending on the cRNAs being tested.

Electrophysiology

Initial recordings were made on a Warner Instruments (Hamden, CT) OC-725C oocyte amplifier and RC-8 recording chamber interfaced to a Macintosh IIcx personal computer, although the majority of experiments employed a Gene Clamp 500 amplifier (Axon Instruments, Foster City, CA) interfaced to a Gateway 2000 (North Sioux City, SD) P5–75 personal computer. Comparable results were obtained on both sets of equipment. Initial experiments were performed in a configuration such that a 2-ml bolus of drug was applied after loading of a loop at the terminus of the drug delivery system, whereas subsequent experiments were conducted in a configuration where drug application was electronically controlled and regulated by duration rather than volume, permitting more rapid solution exchange without stoppage of flow through the chamber. Oocytes were placed in a Lexan recording chamber with a total volume of ~0.6 ml and perfused at room temperature by frog Ringers (115 mM NaCl, 2.5 mM KCl, 10 mM HEPES, pH 7.3, 1.8 mM $CaCl_2$) containing 1 μM atropine to block potential muscarinic responses. A Mariotte flask filled with Ringers was used to maintain a constant hydrostatic pressure for drug deliveries and washes. Drugs were diluted in perfusion solution and applied from a reservoir for 10 s using a two-way electronic valve. Data were acquired using Axoscope 1.1 software (Axon Instruments) at a 20-Hz sample rate and filtered at a rate of 10 Hz using either a CyberAmp 320 external filter (Axon Instruments) or the filter in the amplifier. The rate of drug application was 6 ml/min in all cases. Current electrodes were filled with a solution containing 250 mM CsCl, 250 mM CsF, and 100 mM EGTA and had resistances of 0.5–2 MΩ. Voltage electrodes were filled with 3 M KCl and had resistances of 1–3 MΩ. Oocytes with resting membrane potentials more positive than −30 mV were not used.

Experimental protocol and data analysis

Current responses to drug application were studied under two-electrode voltage clamp at a holding potential of −50 mV unless otherwise noted. Holding currents immediately before agonist application were subtracted from measurements of the peak response to agonist. All drug applications were separated by a wash period for a length of time as noted. At the start of recording, all oocytes received an initial control application of ACh to which subsequent drug applications were normalized to control for the level of channel expression in each oocyte. An experimental application of ACh with inhibitor was followed by an application of ACh alone 10 min after the control ACh application used for normalization. In some receptor subtypes (e.g., $\alpha3\beta4$), rundown was observed to stabilize after a second application of ACh. For these subtypes, responses were normalized to the second of two initial control ACh applications. Means and standard errors (SEMs) were calculated from the normalized responses of at least four oocytes for each experimental concentration.

For all experiments involving use-dependent inhibitors, a concentration of ACh was selected sufficient to stimulate the receptors to a level representing a reasonably high value of p_{open} at the peak of the response, while minimizing rundown with successive ACh applications. For potent use-dependent inhibitors, we have found that this concentration is adequate to achieve maximal inhibition (Francis and Papke, 1996; Papke et al., 1994). Specific concentrations for each receptor subtype are as noted.

For concentration-response relations, data were plotted using Kaleidagraph 3.0.2 (Abelbeck Software, Reading, PA), and curves were generated using the following modified Hill equation (Luetje and Patrick, 1991):

$$\text{Response} = \frac{I_{max}[\text{agonist}]^n}{[\text{agonist}]^n + (\text{EC50})^n} \quad (1)$$

where I_{max} denotes the maximal response for a particular agonist/subunit combination, and n represents the Hill coefficient. I_{max}, n, and the EC50 were all unconstrained for the fitting procedures, and the r values of the fits were all >0.96 (the average r value = 0.97).

For use-dependent inhibitors, measurements of peak response at the time of co-application of agonist with inhibitor underestimate steady-state inhibition in our system. Therefore, in experiments assessing rate of recovery from use-dependent inhibition (see Fig. 2), inhibitor alone was pre-applied for a length of time sufficient to achieve maximal concentration in the chamber before application of agonist. This pre-application protocol maximized the probability of block upon channel activation as a function of inhibitor concentration and permitted the use of peak current as a more accurate measure of steady-state inhibition for applications of ACh in the presence of the TMP compounds. After normalization to the control response (as described above), total inhibition can be calculated by subtracting the normalized value from 1. In this manner, we confirm almost total inhibition at the time of co-application of agonist with inhibitor and are able to generate a recovery rate from this point in time. Agonist concentrations were selected to minimize rundown with successive ACh applications while still providing a high enough probability of channel activation during the time course of a response to achieve close to 100% inhibition and are noted in the figure legend. Recovery rate data were fitted by the following equation:

$$\%\ \text{Inhibition} = I_0(e^{-t/\tau}) \quad (2)$$

which describes a first-order process where I_0 represents the inhibition at time $t = 0$ and τ is the time constant for recovery. The r values of the displayed fits were all >0.96 (the average r value = 0.98).

For experiments assessing voltage dependence of inhibition, oocytes were initially voltage clamped at a holding potential of −50 mV and a control application of ACh alone was delivered. The holding potential was stepped to +20 mV for 30–60 s before co-application of either ACh with bis-TMP-10 or ACh alone. Thirty to sixty seconds after the peak of the co-application response, voltage was stepped back down to −50 mV, and residual inhibition was evaluated with two subsequent applications of ACh alone separated by 5 min.

For experiments assessing protection from long-term inhibition by application of a short-term inhibitor, a saturating concentration of the short-term inhibitor (either QX-314 (lidocaine *N*-ethyl bromide) or TMP) was applied for 30–60 s before the application of ACh and the long-term inhibitor (bis-TMP-10). The application of the short-term inhibitor continued throughout the time course of the co-application of ACh with long-term inhibitor until at least 30 s after the co-application. The concentration of inhibitor and period of application was selected to maximize the potential for protection effects. Recovery from inhibition was evaluated in 3-min intervals after the application of inhibitor in the case of $\alpha1\beta1(\beta4\text{tm2})\gamma\delta$ receptors and 10 min after application of inhibitor in the case of $\alpha3\beta4$ receptors.

Production of tm2 chimeras and sequencing

Chimeric genes were constructed by the method of overlap extension polymerase chain reaction (PCR) (Horton et al., 1989). In brief, the genes $\beta1$ and $\beta4$ were cloned into p-Bluescript SK(−). Specific PCR primers were designed to generate mutants exchanging just the bases necessary to code the tm2 or ecl region. Each primer contained 27 bases of the sequence flanking the tm2 or ecl sequence on one side and 24 bases that coded for the tm2 or ecl region to be exchanged. Oligonucleotides were designed to contain a unique silent restriction site in the mutant region for future screening. Separate PCR reactions consisting of the appropriate PCR primer with template and either T3 or T7 primer selectively amplified the upstream and downstream portions of the gene of interest with overhanging chimeric sequence. These two products were then put together in a second PCR reaction with T3 and T7 primers. The region of chimeric sequence overlap formed double-stranded DNA that primed elongation in both directions, and the full-length product was amplified using T3 and T7 primers. The region coding for the mutant sequence was then cut out with restriction enzymes and cloned back into the original plasmid, reducing the

amount of PCR-generated sequence in the final constructs. Clones were evaluated by both restriction analysis and sequencing through the PCR-generated region by the dideoxy chain termination method (Sanger et al., 1977) using the Sequenase 2.0 kit from United States Biochemical Corp. (Cleveland, OH).

RESULTS

Concentration-response relations of chimeric nAChRs

Chimeric DNAs exchanging sequence coding for eight amino acids of the tm2 region (underlined below) between a neuronal β-subunit (β4) and the muscle β-subunit (β1) were constructed by overlap extension PCR. Following the terminology of Miller (1989) and later Charnet et al. (1991), the tm2 chimeric region extends from position 4′ to position 11′, including the position homologous to the inner polar site of Leonard et al. (1990) at which the charged amino group of the local anesthetic QX-222 has been hypothesized to bind in muscle-type nAChRs (position 6′). The amino acid sequences of the membrane-spanning region, from the intracellular to the extracellular side, are as follows:

	intracellular	MEMBRANE SPANNING II			extracellular
ALPHA1		TDSG*EK	MTLSISVLLSLTVFLLVIVELIPST		
BETA4		SDCG*EK	MTLCISVLLALTFFLLLISKIVPPT		
BETA1		QDAG*EK	MGLSIFALLTLTVFLLLLADKVPET		
			4′ 11′	extracellular loop	
GAMMA		AKAGGQK	CTVATNVLLAQTVFLFLVAKKVPET		
DELTA		GDCG*EK	TSVAISVLLAQSVFLLLISKRLPAT		

These chimeric β-subunits were then expressed with the other muscle subunits (α1,γ,δ) to produce $\alpha1\beta1(\beta4tm2)\gamma\delta$ and $\alpha1\beta4(\beta1tm2)\gamma\delta$ receptors. The effects of these exchanges were initially evaluated in the muscle receptor because only a single β-subunit is included per receptor, whereas neuronal nAChRs include multiple β-subunits. The presence of a single neuronal β-subunit in combination with the other muscle subunits has been previously shown to be sufficient for achieving long-term inhibition after co-application of bis-TMP-10 with ACh (Papke et al., 1994).

Co-injection of chimeric or wild-type β-subunit RNA with RNA coding for the other muscle subunits provides for the expression of functional $\alpha1\beta1\gamma\delta$, $\alpha1\beta4\gamma\delta$, $\alpha1\beta1(\beta4tm2)\gamma\delta$, and $\alpha1\beta4(\beta1tm2)\gamma\delta$ receptors with activation profiles typical of nAChRs. To interpret data comparing the magnitude of use-dependent inhibition across receptor subtypes, it is necessary to first define a relationship between the experimental concentration of agonist applied and the EC50 for each receptor subtype. Although the EC50s for each of the receptor subtypes differ somewhat, the Hill coefficients for all of the receptor subtypes are in the range of 1–2, typical of nAChRs. Although $\alpha1\beta1\gamma\delta$, $\alpha1\beta4\gamma\delta$, and $\alpha1\beta4(\beta1tm2)\gamma\delta$ receptors show comparable EC50s (in the range of 3–8 μM), $\alpha1\beta1(\beta4tm2)\gamma\delta$ receptors require approximately a fivefold higher concentration of ACh (30 μM) for 50% activation. The concentration of ACh used in specific experiments ranges between 5 and 30 μM depending on receptor type or experimental design and is noted in the figure legends.

Dependence of long-term inhibition by bis-TMP-10 on sequence in the tm2 region

The time course of recovery from inhibition by bis-TMP-10 was examined for a number of different subunit combinations (Fig. 1). Although normal muscle-type receptors con-

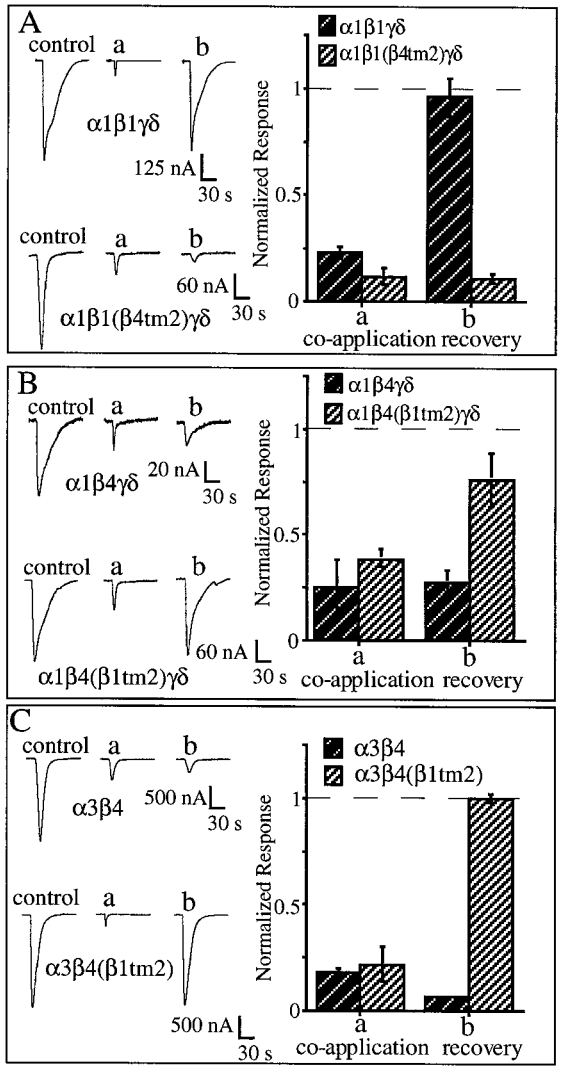

FIGURE 1 β-Subunit tm2 exchange has reciprocal effects on the duration of inhibition by bis-TMP-10. In each panel, traces representative of the mean data are shown on the left. The trace marked *a* is the response to a co-application of ACh with inhibitor, and the trace marked *b* is the response to ACh alone 5 min later and is used as a measure of recovery from inhibition. To generate mean data, the co-application (*a*) and recovery (*b*) responses are normalized to the trace marked control. Mean data are displayed in the bar graphs on the right. In each graph, the pair of bars on the left (*a*) represent the normalized response to a co-application of ACh with 2 μM bis-TMP-10 and correspond to the trace marked *a* at left. The pair of bars on the right (*b*) represent the normalized response to an application of ACh alone 5 min after the co-application response and correspond to the trace marked *b* at left. Each column represents the mean response ± SEM of at least four oocytes injected with RNA coding for either: (*A*) $\alpha1\beta1\gamma\delta$ (■) or $\alpha\beta1(\beta4tm2)\gamma\delta$ (▨); (*B*) $\alpha1\beta4\gamma\delta$ (■) or $\alpha1\beta4(\beta1tm2)\gamma\delta$ (▨); (*C*) $\alpha3\beta4$ (■) or $\alpha3\beta4(\beta1tm2)$ (▨) nAChRs. The concentration of ACh in each experiment is either 30 μM (*A* and *B*) or 100 μM (*C*). All responses are separated by 5-min wash intervals.

sistently recover from inhibition within 5 min after co-application of 30 μM ACh and 2 μM inhibitor, $\alpha1\beta1(\beta4tm2)\gamma\delta$ chimeric receptors show more prolonged inhibition (Fig. 1 *A*). To demonstrate a reciprocal dependence of this effect, the time course of recovery from inhibition of $\alpha1\beta4\gamma\delta$ receptors after co-application of 2 μM bis-TMP-10 and 30 μM ACh was compared with that of $\alpha1\beta4(\beta1tm2)\gamma\delta$ receptors (Fig. 1 *B*). Whereas $\alpha1\beta4\gamma\delta$ receptors remain ~73% inhibited after 5 min, $\alpha1\beta4(\beta1tm2)\gamma\delta$ receptors recover to near control levels. Additionally, coexpression of the neuronal $\alpha3$ subunit with the chimeric $\beta4(\beta1tm2)$ subunit produces receptors that recover completely from inhibition within 5 min, whereas normal $\alpha3\beta4$ receptors are still ~93% inhibited (Fig. 1 *C*). It should also be noted that continuous application of 2 μM bis-TMP-10 to $\alpha1\beta4(\beta1tm2)\gamma\delta$ receptors for up to 1 min in duration without co-application of agonist does not produce any significant inhibitory effects, indicating the use dependence of inhibition (data not shown).

The rapid recovery of $\alpha3\beta4(\beta1tm2)$ receptors from inhibition by bis-TMP-10 indicates that the neuronal $\alpha3$ subunit is insensitive to long-term inhibition after application of bis-TMP-10. The sensitivities of the neuronal $\alpha2$ and $\alpha4$ subunits to inhibition by bis-TMP-10 were also evaluated. Although attempts to get expression of $\alpha4\beta4(\beta1tm2)$ receptors were unsuccessful, $\alpha2\beta4(\beta1tm2)$ receptors recover completely within 5 min from the inhibition elicited with co-application of 30 μM ACh and 2 μM bis-TMP-10 (data not shown). As the $\alpha4$ and $\alpha2$ subunits are identical within the tm2 domains, it is hypothesized that α-subunits do not play a role in determining sensitivity to long-term inhibition by bis-TMP-10.

A chimeric β-subunit in which a sequence from the putative ecl region between tm2 and tm3 of a neuronal $\beta4$ subunit was replaced with the homologous sequence from the muscle $\beta1$ subunit (shown in bold above) was also constructed. The bis-TMP-10 sensitivity of receptors resulting from coexpression of the $\beta4(\beta1ecl)$ subunit with either the other muscle subunits (α, γ, and δ) or the neuronal $\alpha3$ subunit was evaluated. The substitution of the $\beta1$ ecl sequence does not reverse the long-term inhibition normally observed with co-application of bis-TMP-10 and ACh to either the $\alpha1\beta4\gamma\delta$ or $\alpha3\beta4$ subunit combinations. Five minutes after co-application of 2 μM bis-TMP-10 with an appropriate concentration of ACh (10 or 100 μM, respectively), the responses of $\alpha1\beta4(\beta1ecl)\gamma\delta$ ($n = 3$) and $\alpha3\beta4(\beta1ecl)$ receptors ($n = 4$) recover to only 13 $\pm$ 02% and 7 $\pm$ 01% of initial control responses to ACh alone (data not shown).

To examine the rate of recovery from inhibition for individual receptor subtypes, ACh was applied at time points beyond 5 min after co-application of ACh with bis-TMP-10 and residual inhibition was evaluated (Fig. 2). For these experiments, 2 μM bis-TMP-10 alone was applied continuously for 15–20 s before application of ACh in the continued presence of 2 μM bis-TMP-10. The ACh concentrations used were either 10 μM for the $\alpha1\beta1\gamma\delta$, $\alpha1\beta4\gamma\delta$, $\alpha1\beta1(\beta4tm2)\gamma\delta$, or $\alpha1\beta4(\beta1tm2)\gamma\delta$ subunit combinations or 100 μM ACh for $\alpha3\beta4$ receptors. Muscle-type receptors show the most rapid recovery from inhibition with a time constant of recovery (τ_r) of ~3 min, whereas chimeric $\alpha1\beta1(\beta4tm2)\gamma\delta$ receptors exhibit the most prolonged inhibition (τ_r = 81 min). As expected, $\alpha3\beta4$ receptors also show prolonged inhibition with a time constant of recovery of ~70 min. The rate of recovery of $\alpha1\beta4(\beta1tm2)\gamma\delta$ receptors (τ_r = 6 min) is most comparable to that of muscle-type receptors, whereas the recovery rate of $\alpha1\beta4\gamma\delta$ receptors falls in an intermediate range (τ_r = 16 min).

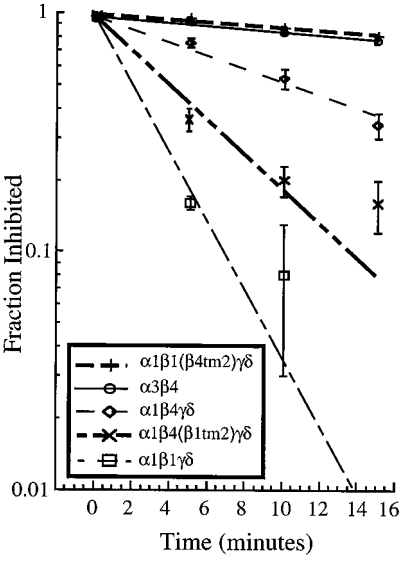

FIGURE 2 Recovery from inhibition by bis-TMP-10 as a function of time. The data points at $t = 0$ min represent a measure of total inhibition observed after co-application of ACh with 2 μM bis-TMP-10 (see Materials and Methods). Data points at $t = 5$, $t = 10$, or $t = 15$ min represent mean values of residual inhibition measured after application of ACh alone. For $\alpha1\beta1\gamma\delta$ receptors, full recovery was effectively achieved after only 10 min of wash, so the data at the 15-min time point for this receptor subtype is omitted for clarity. All drug applications are separated by 5-min wash periods. The concentration of ACh in each experiment is either 10 μM ($\alpha1\beta1\gamma\delta$, $\alpha\beta1(\beta4tm2)\gamma\delta$, $\alpha1\beta4\gamma\delta$, and $\alpha1\beta4(\beta1tm2)\gamma\delta$) or 100 μM ($\alpha3\beta4$ and $\alpha3\beta4(\beta1tm2)$. All data points represent the mean responses of at least four oocytes and are fit with an equation describing exponential recovery (see Materials and Methods). In some cases (e.g., $\alpha1\beta1\gamma\delta$), the recovery process appears to contain two components. However, the normalized responses at later time points reflect the minimal contribution of response rundown over time.

Inhibition is independent of voltage

As the residence time of the previously characterized open-channel blockers QX-222 and QX-314 has been shown to be dependent on membrane voltage (Leonard et al., 1988; Neher and Steinbach, 1978) and block by a variety of bis-ammonium compounds has also been shown to be voltage-dependent (Ascher et al., 1979; Bertrand et al., 1990; Zhorov et al., 1991), we hypothesized that inhibition by bis-TMP-10 should also show voltage dependence if inhibition occurs via binding to the chimeric tm2 region directly.

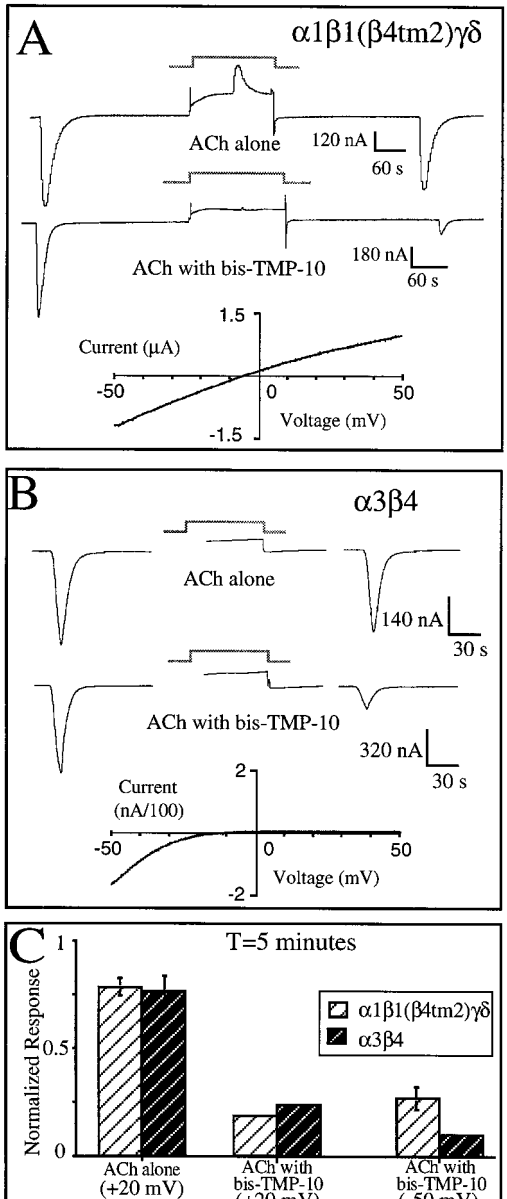

FIGURE 3 Long-term inhibition of either $\alpha1\beta1(\beta4tm2)\gamma\delta$ (*A*) or $\alpha3\beta4$ (*B*) receptors by bis-TMP-10 is independent of voltage. In the representative traces of *A* and *B*, an initial control application of either 30 μM (*A*) or 100 μM (*B*) ACh is followed by either successive applications of ACh alone (*upper trace*) or by a single co-application of ACh with 2 μM bis-TMP-10 followed by subsequent application of ACh alone (*lower trace*). The timing of the voltage step from −50 mV to +20 mV is represented by ▬ and begins ~30 s before and ends ~30 s after the peak of the co-application response in each case. Five-minute wash periods separate each response. Representative current-voltage relationships for each of these receptor subtypes during the plateau phase of the response to extended application of either 30 or 100 μM ACh are also shown. As measured from the *I-V* relationships, the mean reversal potential for $\alpha1\beta1(\beta4tm2)\gamma\delta$ receptors is -4.0 ± 2.1 mV ($n = 3$) and for $\alpha3\beta4$ receptors is -11.0 ± 2.3 mV ($n = 4$). Holding currents during ramps in the absence of agonist were point to point subtracted. In *C*, mean normalized data for the 5-min time point (corresponding to traces at far right in *A* and *B* above) are shown. Each pair of bars represents the normalized response of either $\alpha1\beta1(\beta4tm2)\gamma\delta$ (▨) or $\alpha3\beta4$ (▩) receptors to application of either 30 μM ($\alpha1\beta1(\beta4tm2)\gamma\delta$) or 100 μM ($\alpha3\beta4$) ACh alone at a holding potential of −50 mV 5 min after one of three experimental conditions, from left to right: 1) application of ACh alone during a voltage step to +20 mV, 2) co-application of ACh with bis-TMP-10 during a voltage step to +20 mV, or 3) co-application of ACh with bis-TMP-10 at a constant holding potential of −50 mV.

As $\alpha1\beta1(\beta4tm2)\gamma\delta$ receptors resemble neuronal nAChRs in their time course of recovery from inhibition but maintain the linear current-voltage relationship typical of muscle-type nAChRs (Fig. 3 *A*, bottom), it is possible to examine the effects of voltage on sensitivity to inhibition independent of voltage effects on channel gating. A voltage step to +20 mV for the duration of the co-application of 30 μM ACh with 2 μM bis-TMP-10 does not increase the rate of recovery of $\alpha1\beta1(\beta4tm2)\gamma\delta$ receptors from inhibition or significantly reduce the relative magnitude of inhibition from that observed with a steady holding potential of −50 mV (Fig. 3, *A* and *C*). Thus, the binding of bis-TMP-10 to its activation-sensitive site appears to be independent of membrane voltage in $\alpha1\beta1(\beta4tm2)\gamma\delta$ receptors.

The same paradigm was used to examine the dependence of inhibition on membrane voltage for the $\alpha3\beta4$ receptor subtype (Fig. 3 *B*). However, as neuronal receptors show pronounced inward rectification (Fig. 3 *B*, bottom), a lack of inhibition at positive potentials may result from either a voltage dependence of inhibition itself or a voltage dependence for channel opening. Although neuronal nAChRs pass very little outward current at depolarized potentials, a co-application of 100 μM ACh with 2 μM bis-TMP-10 during a voltage step to +20 mV produces ~75% residual inhibition as assessed with application of ACh alone at a holding potential of −50 mV 5 min after co-application of inhibitor with ACh (Fig. 3 *B*, lower trace, and Fig. 3 *C*). This inhibition is clearly independent of the minimal run-down observed with control applications of ACh alone (Fig. 3 *B*, upper trace).

Open-channel blockers do not protect nAChRs from long-term inhibition by bis-TMP-10

Although the β-subunit tm2 chimeras demonstrate a dependence of inhibition on sequence in the tm2 region, the lack of voltage dependence for this inhibition suggests an indirect effect of the tm2 region rather than binding of the inhibitor directly to this region. We hypothesized that, if bis-TMP-10 binds to the tm2 region directly, a pre-application of the previously characterized open-channel blocker lidocaine *N*-ethyl bromide (QX-314) should protect from long-term inhibition. To evaluate this hypothesis for chimeric $\alpha1\beta1(\beta4tm2)\gamma\delta$ receptors, we applied 100 μM QX-314 alone continuously for 1 min before and throughout a 10-s co-application of 2 μM bis-TMP-10 with 5 μM ACh until 1 min after the co-application of agonist and long-term inhibitor (Fig. 4 *A*). Residual inhibition was then evaluated with applications of ACh alone at 3 and 6 min after co-application of ACh with inhibitor (Fig. 4, *A* and *C*). Al-

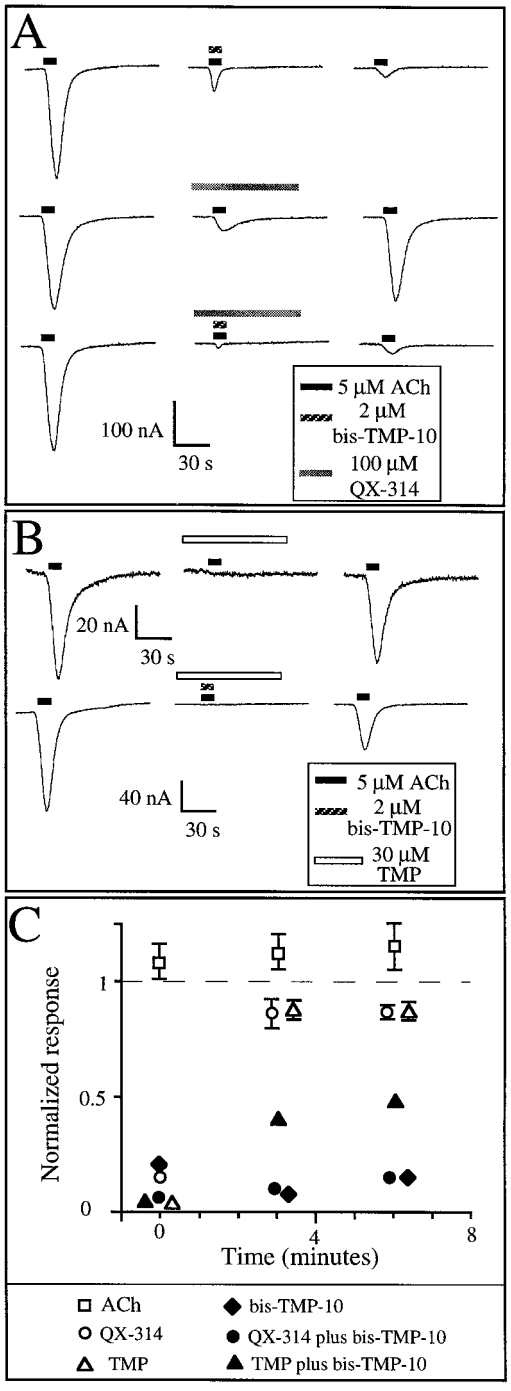

FIGURE 4 Effects of presence of short-term inhibitors on long-term inhibition of $\alpha1\beta1(\beta4tm2)\gamma\delta$ receptors. In the representative traces of *A* and *B*, the thick lines above the traces indicate the duration of agonist and/or inhibitor application. In each set of three traces of *A*, the first trace (from left) represents the response to a 10-s application of 5 μM ACh (—), whereas the second trace (from left) represents the response to either a co-application of 5 μM ACh with 2 μM bis-TMP-10 (—, upper), an application of 5 μM ACh in the continued presence of 100 μM QX-314 (—, middle), or 5 μM ACh co-applied with 2 μM bis-TMP-10 in the continued presence of 100 μM QX-314 (lower). In each set of three traces of *B*, the first trace (from left) represents the response to 5 μM ACh, whereas the second trace (from left) represents the response to either an application of 5 μM ACh in the continued presence of 30 μM TMP (—, upper) or a co-application of 5 μM ACh with 2 μM bis-TMP-10 in the continued presence of 30 μM TMP (lower). In all cases, the third trace (from left) represents the response to ACh alone applied after a 3-min wash period. The scatter plot in *C* displays the mean normalized responses ± SEM of at least four oocytes as a function of time. The points at $t = 0$ min correspond to the second trace (from left) in each of the sets of traces above: bis-TMP-10 with ACh (♦), QX-314 with ACh (○), ACh with QX-314 and bis-TMP-10 (●), TMP with ACh (△), and ACh with TMP and bis-TMP-10 (▲); □, the response to successive applications of ACh alone. The data points at 3 and 6 min show the mean responses to ACh alone after washout of inhibitor and are used as measures of recovery from inhibition. Overlapping plot symbols were shifted by ~30 s to aid in the viewing of all data points.

though this receptor subtype consistently recovers within 3 min from inhibition elicited using the same application paradigm without the bis-TMP-10 application (middle trace), co-application of bis-TMP-10 in the presence of QX-314 consistently produces long-term inhibition (~90% at $t = 3$ min) that is not significantly different from control applications of bis-TMP-10 with ACh (compare upper and lower traces). These results demonstrate a lack of effect of QX-314 on inhibition by bis-TMP-10. However, because of the potential for multiple intraburst blocking and unblocking events during the time course of agonist application in the presence of the short-term inhibitor, we also repeated the experiment at higher concentrations of QX-314 (up to 500 μM) and at more negative potentials. No protection from long-term inhibition was observed with voltage steps to −80 mV or applications of 500 μM QX-314 ($n = 3$; data not shown).

The effects of the monofunctional inhibitor TMP (30 μM) on long-term inhibition of $\alpha1\beta1(\beta4tm2)\gamma\delta$ receptors were also evaluated using the same application paradigm (Fig. 4 *B*). TMP is able to produce ~30% protection from long-term inhibition. These results are summarized in Fig. 4 *C*.

A similar set of experiments was conducted on the $\alpha3\beta4$ receptor subtype. The co-application of short- and long-term inhibitors was conducted in the same manner as described above. Application of 500 μM QX-314 produces a small amount of protection (~18%) from long-term inhibition by bis-TMP-10 (Fig. 5 *A*), whereas application of 4 μM TMP with bis-TMP-10 (Fig. 5 *B*) limits long-term inhibition to a level that is not significantly different from that observed with application of only the short-term inhibitor TMP. These results are summarized in Fig. 5 *C*.

Long-term inhibition is dependent upon compound length

If binding of both TMP moieties of the bifunctional compounds is necessary for long-term inhibition, we reasoned that the distance between TMP moieties might represent a constraint on inhibitory activity. To test this hypothesis, the amount of inhibition remaining at time points 5 and 10 min after co-application of inhibitor with ACh to either chimeric $\alpha1\beta1(\beta4tm2)\gamma\delta$ or neuronal $\alpha3\beta4$ receptors was assessed

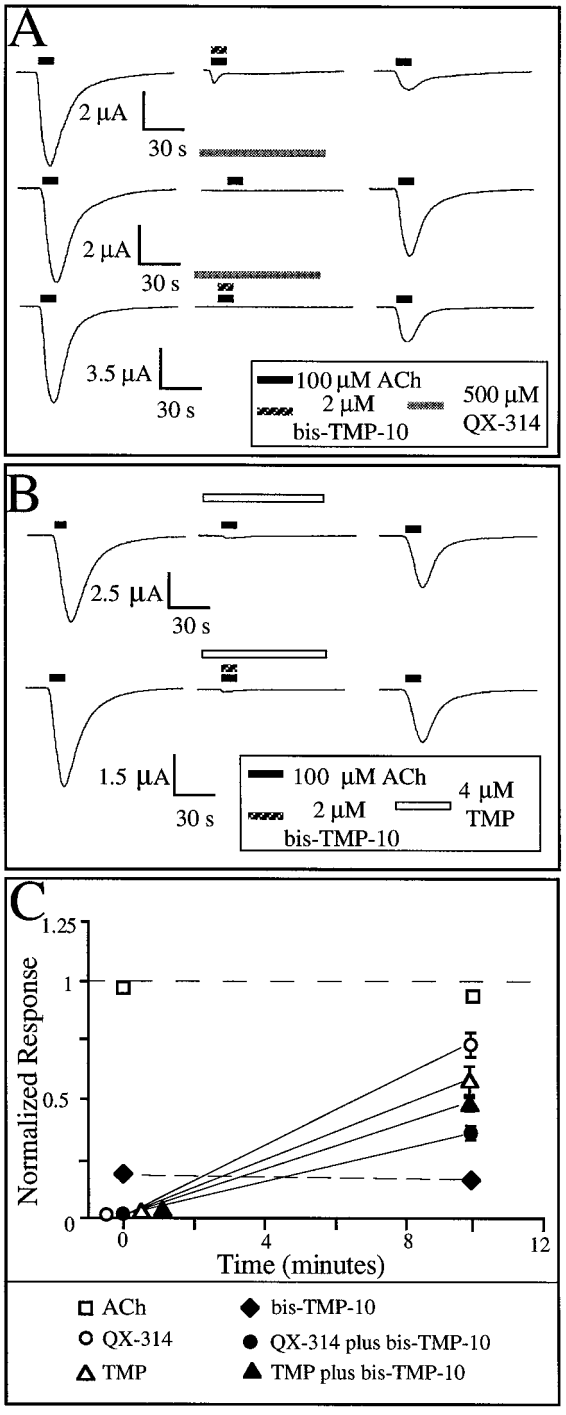

FIGURE 5 Effects of presence of short-term inhibitors on long-term inhibition of $\alpha 3\beta 4$ receptors. In the representative traces of *A* and *B*, the thick lines above the traces indicate the duration of agonist and/or inhibitor application. In each set of three traces of *A*, the first trace (from left) represents the response to a 10-s application of 100 μM ACh (▬), whereas the second trace (from left) represents the response to either a co-application of 100 μM ACh with 2 μM bis-TMP-10 (▬, upper), an application of 100 μM ACh in the continued presence of 500 μM QX-314 (▬, middle), or 100 μM ACh co-applied with 2 μM bis-TMP-10 in the continued presence of 500 μM QX-314 (lower). In each set of three traces of *B*, the first trace (from left) represents the response to 100 μM ACh, whereas the second trace (from left) represents the response to either an application of 100 μM ACh in the continued presence of 4 μM TMP (▬, upper trace) or a co-application of 100 μM ACh with 2 μM bis-TMP-10 in the continued presence of 4 μM TMP (lower trace). In all cases, the third trace (from left) represents the response to an application of 100 μM ACh alone after a 10-min wash period. The scatter plot in *C* displays the mean normalized responses ± SEM of at least four oocytes as a function of time. The points at $t = 0$ min correspond to the second trace (from left) in each of the sets of traces above: bis-TMP-10 with ACh ([♦), QX-314 with ACh ([○), ACh with QX-314 and bis-TMP-10 (●), TMP with ACh (△), and ACh with TMP and bis-TMP-10 (▲); □, the response to successive applications of ACh alone. The data points at 10 min show the mean responses to ACh alone after washout of inhibitor and are used as measures of recovery from inhibition. Overlapping plot symbols at $t = 0$ min were shifted in time to aid in the viewing of all data points.

for bifunctional TMP molecules differing only in the length of their carbon linker. TMP, bis-TMP-4, bis-TMP-6, bis-TMP-8, bis-TMP-10, and bis-TMP-12 were tested for their inhibitory effects (Fig. 6). For both receptor subtypes, all of the compounds, including the monofunctional inhibitor TMP, show some inhibitory activity at the time of co-application with ACh. However, no significant residual inhibition of $\alpha 1\beta 1(\beta 4\text{tm2})\gamma\delta$ receptors results from co-application with ACh of compounds with linkers of eight carbons or less whereas pronounced residual inhibition is present after application of inhibitors with linkers of 10 or more carbons. In contrast, for neuronal nAChRs ($\alpha 3\beta 4$), all bifunctional compounds show some degree of residual inhibitory activity at time points 5 and 10 min after the time of co-application with ACh (Fig. 6, bottom), and the magnitude of residual inhibition increases with increasing compound length. These results are consistent with binding of each of the piperidinyl groups to distinct sites separated by a characteristic length specific to each subunit combination.

Based on previous work demonstrating that the δ-subunit of muscle-type nAChRs is sensitive to the TMP moiety (Francis and Papke, 1996), we reasoned that distinct sites might be represented on separate subunits. To demonstrate a requirement for contributions by at least two TMP-sensitive subunits for long-term inhibition, it was necessary to examine the time course of recovery from inhibition of receptors containing only a single sensitive subunit. $\alpha 1\beta 1(\beta 4\text{tm2})\gamma$ receptors show no measurable residual inhibition 5 min after co-application of 30 μM ACh with 2 μM bis-TMP-8 ($n = 4$) or 2 μM bis-TMP-10 ($n = 6$; data not shown).

DISCUSSION

A great deal of research has employed the use of noncompetitive inhibitors to explore the relationship between structure and function in ion channels. The muscle-type/*Torpedo* nAChR is the prototype system for these studies both because of its ready availability in purifiable quantities and the rigorous characterization of its functional role at the neuromuscular junction. By examining the mechanism of inhibition of a class of drugs that show selectivity for the long-term inhibition of neuronal nAChRs, we attempt to extend the analysis of structure-function relationships to neuronal

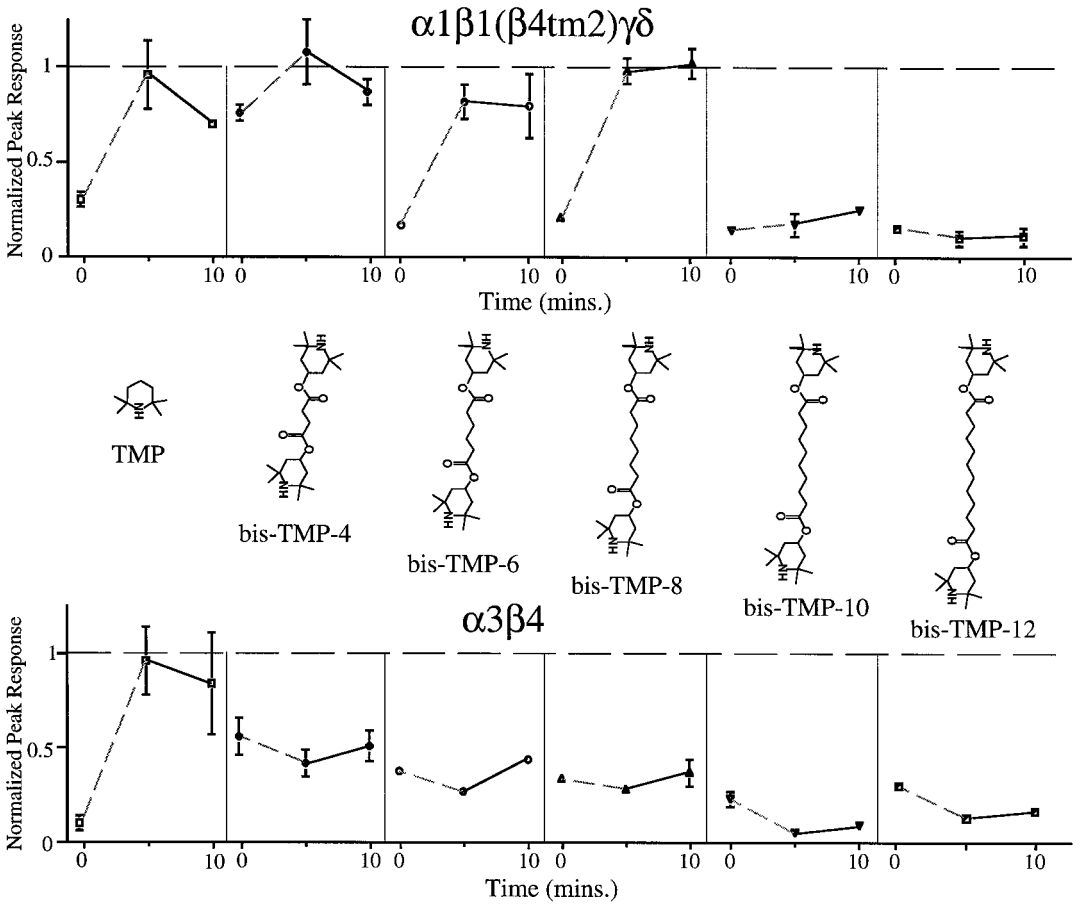

FIGURE 6 The effects of compound length on long-term inhibition of $\alpha1\beta1(\beta4tm2)\gamma\delta$ and $\alpha3\beta4$ nAChRs. All data points represent the mean peak response ± SEM of at least four oocytes normalized to an initial control response to ACh alone. In each graph, the data point at $t = 0$ min represents the normalized response to co-application of either a 4 μM concentration of the monofunctional compound (TMP, left) or a 2 μM concentration of the bifunctional compounds with 30 μM ACh. The data points at $t = 5$ and $t = 10$ min represent the normalized responses to 30 μM ACh alone after washout of inhibitor and are used as measures of recovery from inhibition. It should be noted that, in these experiments, measures of relative inhibition of peak current at $t = 0$ min do not quantitate steady-state inhibition (see Materials and Methods) but serve to demonstrate the fundamental sensitivity of both receptor subtypes to the TMP compounds. For this reason, the data points at $t = 0$ min are connected to the 5-min data points by a dashed line.

nAChRs. Interestingly, our data demonstrate that long-term inhibition is strictly use dependent within the time frame of our application of inhibitor but apparently not associated with direct binding to site(s) situated within the portion of the ion channel pore influenced by the membrane electric field. The most parsimonious interpretation of these data allows for interactions upon channel activation between residues located within the tm2 region of neuronal β-subunits and sequence elements situated outside of the membrane electric field. It is possible that these interactions, in turn, result in the exposure of the use-dependent binding site(s) for bis-TMP-10.

TM2 determines kinetics of long-term inhibition

Our studies examining the time course of inhibition of receptors containing chimeric β-subunits localize the major structural determinant of sensitivity to long-term inhibition to an eight-amino-acid stretch of neuronal β-subunits. All receptor subtypes tested that incorporate the neuronal β-subunit tm2 region paired with either a second neuronal β-subunit (neuronal nAChRs) or a δ-subunit (neuronal-muscle chimeras) exhibit a significant degree of residual inhibition as measured at time points 5 min or more after the co-application of agonist with inhibitor. The reversal of long-term inhibition upon substitution of the $\beta1$ subunit tm2 region for the $\beta4$ subunit tm2 region in $\alpha1\beta4(\beta1tm2)\gamma\delta$ and $\alpha3\beta4(\beta1tm2)$ receptors in conjunction with the observation that substitution of the $\beta1$ ecl region does not reverse long-term inhibition demonstrates this effect to be specific for the tm2 region. Although $\alpha1\beta4\gamma\delta$ receptors exhibit prolonged inhibition compared with $\alpha1\beta4(\beta1tm2)\gamma\delta$ or muscle-type receptors (Fig. 2), they recover from inhibition more rapidly than the $\alpha1\beta1(\beta4tm2)\gamma\delta$ or $\alpha1\beta4(\beta1ecl)\gamma\delta$ receptor subtypes. Taken together, these observations perhaps suggest that, when associated with the other muscle subunits in $\alpha1\beta4\gamma\delta$ receptors, regions of the $\beta4$ subunit not contained within the tm2 domain may affect the binding of inhibitor directly or otherwise allow for increased recovery rate. The $\beta4$ subunit has been shown to confer the property

of prolonged burst kinetics upon the neuronal subunits with which it is expressed (Papke and Heinemann, 1991). It may be the case that activation properties such as burst duration or channel open time, which may be specific to individual receptor subtypes, can also influence recovery rate or the probability of block as a function of peak current.

Significance of voltage-independent inhibition

In contrast to studies on the open-channel blockers QX-222 and QX-314 (Neher and Steinbach, 1978) and studies on the symmetrical bis-ammonium series of ganglionic blockers (Ascher et al., 1979) in which block has been shown to be dependent on membrane potential, the inhibition by bis-TMP-10 seems to be independent of voltage. The lack of voltage dependence for inhibition brings to mind two possibilities: either the noncompetitive binding site is outside of the membrane electric field or bis-TMP-10 is uncharged at physiological pH. Although direct evaluation of the pK_a of bis-TMP-10 has not been possible because of solubility limitations, it is known that the monofunctional inhibitor TMP has a pKa in the range of 10–11 (Perrin, 1965). The pKa of simple bis-amino compounds are reduced if the amines are separated by short (two to four) carbon chains. However, when the amines are separated by a longer (e.g., eight) carbon chain, the pKa values of the two ionizable groups both approach that of the monofunctional amine. Therefore, with the pKa of the monofunctional piperidine in the range of 10–11, it is unlikely that the lower of the 2 pKa values of the bis compound would be under 9–10. Thus, at physiological pH, both functional groups should be predominantly charged.

The voltage-independent long-term inhibition of $\alpha3\beta4$ receptors is particularly intriguing. As shown in Fig. 3 *C*, the inhibition observed 5 min after the co-application of agonist with inhibitor at +20 mV (~75%) is slightly less than that typically observed 5 min after co-applications of ACh with bis-TMP-10 at −50 mV (~90%). This effect may represent a voltage-dependent component of long-term inhibition but more likely represents an effect of the voltage dependence of channel gating independent of any voltage dependence for inhibition. In either case, at this potential, no outward current was measured in response to control applications of ACh alone, implying that the activation-dependent state associated with inhibition is distinct from the conducting state. The inward rectification of neuronal nAChRs is due, at least in part, to a magnesium block dependent upon the sequence at the cytosolic mouth of the channel (Ifune and Steinbach, 1992; Imoto et al., 1988; Sands and Barish, 1992). Our data suggest that a gating conformation may still be present at depolarized potentials and are consistent with channel block by magnesium from the intracellular side. Thus, bis-TMP-10 appears to be able to produce long-term inhibition of neuronal nAChRs that are gated (or activated) but nonconducting as a result of block from the intracellular side. Alternatively, it may be the case that a high-affinity desensitized state is favored at depolarized potentials in the presence of agonist. Our data would suggest that a gated conformation is associated with this state as well.

We also tested the hypothesis that bis-TMP-10 can produce long-term inhibition in nAChRs that are nonconducting as a result of blockade from the extracellular side. We chose to use the open-channel blocker QX-314 in these experiments based upon three criteria: 1) the QX-314 binding site is believed to be located approximately three-fourths of the way across the membrane electric field, and thus inhibition by this compound is voltage dependent (Neher and Steinbach, 1978); 2) QX-314 has been shown to interact with residues at homologous positions to those contained within the region of our β-subunit tm2 chimeras (Pascual and Karlin, 1997); and 3) QX-314 has a longer residence time in the pore than the structurally related local anesthetic QX-222 (Neher and Steinbach, 1978). In addition, studies in our laboratory have shown that the inhibition of chimeric $\alpha1\beta1(\beta4tm2)\gamma\delta$ receptors by QX-314 is voltage dependent, indicating that, for this subunit combination also, the QX-314 binding site is located within the membrane electric field (M.M. Francis and R.L. Papke, unpublished observations).

For $\alpha1\beta1(\beta4tm2)\gamma\delta$ receptors, the lack of an effect of even very high concentrations of QX-314 (500 μM) on the magnitude of residual inhibition after co-application of bis-TMP-10 with ACh is consistent with the observed voltage independence of inhibition by bis TMP-10. For $\alpha3\beta4$ receptors, QX-314 does produce a detectable reduction in the magnitude of residual inhibition (Fig. 5 *C*). This observation suggests that in this subunit combination the sites of action for bis-TMP-10 and QX-314 are not totally independent. From our data, it is difficult to ascertain whether the partial protection we observe represents interactions of both drugs at a single site or, alternatively, an allosteric interaction between two distinct sites, such that the binding of QX-314 decreases the gating-dependent changes at the site of TMP binding.

For both receptor subtypes, the short-term inhibitor TMP produces a significantly greater degree of protection from long-term inhibition than was observed with QX-314. This finding demonstrates a degree of overlap in the sites of action between the mono- and bifunctional compounds. The lack of complete protection may suggest a contribution of the hydrophobic linker region in stabilizing bis-TMP-10 binding or may indicate that a different subset of binding sites are available to the smaller TMP compound. The latter hypothesis is supported by the observation of a slight voltage dependence for inhibition by TMP (Papke et al., 1994).

Significance of compound length requirement for long-term inhibition

We have previously shown that $\alpha\beta\delta$ receptors are sensitive to long-term inhibition by bis-TMP-10. Based on these data, we hypothesized that a TMP binding site is present on the δ-subunit of muscle-type nAChRs and that long-term inhibition occurs via interactions at multiple sites (Francis and

Papke, 1996). Consistent with this hypothesis, we now present data that suggest that substitution of the muscle β-subunit tm2 sequence with the neuronal β-subunit tm2 sequence results in the exposure of a second TMP binding site located outside of the membrane electric field. Furthermore, because long-term inhibition is dependent upon the sequence in tm2 for both chimeric muscle and chimeric neuronal receptors, it seems reasonable that the inhibitor binding site may represent a structural motif that is conserved across classes of β-subunits. For the β-subunit of muscle-type nAChRs, it has been shown that channel activation alters the accessibility of substituted cysteines at positions immediately extracellular to the region of our chimera (Zhang and Karlin, 1996). It may be the case that these residues contribute to a binding site for bis-TMP-10.

The results of both the voltage dependence and protection experiments localize the majority of bis-TMP-10 effects to sites lying outside the membrane electric field. Given the data, it seems logical to speculate that these sites lie on the extracellular portion of the receptor, possibly as a part of the protein domains forming the extracellular vestibule. In its most extended conformation, bis-TMP-10 is estimated to have a length of between 20 and 23 Å. This estimate of length is consistent with binding to sites on separate subunits in the wider, extracellular portion of the channel. Nonetheless, it may be the case that, in addition to tethering the piperidinyl groups, the flexible linker region of the bis-TMP compounds serves to stabilize binding via hydrophobic interactions, and differences in this form of interaction could underlie some of the sensitivity differences between the chimeras and the neuronal receptors. The relative importance of hydrophobic versus polar groups in stabilizing the interactions between bis-TMP-10 and its binding site(s) is currently under investigation, and these data will be presented elsewhere.

If the primary function of the linker region is to serve as a tether between active inhibitory moieties, then the differences in size constraints may provide some insight into the disposition of sensitive subunits within a receptor complex. Although a number of studies have provided evidence that the δ-subunit is situated adjacent to the β-subunit in *Torpedo* nAChRs (Holtzman et al., 1981; Karlin et al., 1983; Machold et al., 1995), comparable data are lacking for muscle receptors, either in vivo or in heterologous expression systems. Our results demonstrate that both a minimal 10-carbon distance between TMP moieties and the presence of the δ-subunit are required for effective long-term inhibition of $\alpha1\beta1(\beta4tm2)\gamma\delta$ receptors. In contrast to the less stringent length requirement for long-term inhibition of neuronal receptors, the requirement for a long linker to achieve long-term inhibition of $\alpha1\beta1(\beta4tm2)\gamma\delta$ receptors seems most consistent with a model in which the distance between the TMP moieties of an extended conformation of bis-TMP-10 represents the distance between opposing rather than adjacent β- and δ-subunits. However, our data to this point cannot absolutely rule out the alternative possibility that the inhibitor binds to asymmetrically disposed sites on adjacent subunits.

In summary, our results demonstrate that the selective long-term inhibition of neuronal nicotinic receptors by bis-TMP-10 is dependent upon the sequence in the tm2 region. We show, however, that long-term inhibition is apparently independent of binding to this region directly. Because inhibition depends upon previous activation of the channel, our results imply that bis-TMP-10 binds to a structural element that may become available as a result of the conformational change associated with channel gating. The observed compound length requirements are consistent with binding to an extracellular site. Future studies employing this class of inhibitors and functional analogs in conjunction with other techniques may add unique insights to the structural changes that take place with channel gating.

Rat nicotinic receptor cDNAs were generously provided by Drs. Jim Boulter and Steve Heinemann of the Salk Institute. We thank Dr. Arthur Karlin for helpful scientific discussion. We thank Dr. Jeffrey K. Harrison for the use of equipment and Mina Salafranca for technical aid in DNA sequencing. We also thank Ricardo Quintana and Wayne Gottlieb for design and synthesis of chimeric DNAs and Amy Poirier, James Friske, and Jeff Thinschmidt for aid in data acquisition.

This work was supported by National Institutes of Health grant NS32888 to R.L. Papke. M.M. Francis was supported by National Institutes of Mental Health grant MH11258.

REFERENCES

Akabas, M. H., C. Kaufmann, P. Archdeacon, and A. Karlin. 1994. Identification of acetylcholine receptor channel-lining residues in the entire M2 segment of the alpha subunit. *Neuron.* 13:919–927.

Akabas, M. H., D. A. Stauffer, M. Xu, and A. Karlin. 1992. Acetylcholine receptor channel structure probed in cysteine-substitution mutants. *Science.* 258:307–310.

Anand, R., W. G. Conroy, R. Schoepfer, P. Whiting, and J Lindstrom. 1991. Neuronal nicotinic acetylcholine receptors expressed in *Xenopus* oocytes have a pentameric quaternary structure. *J Biol. Chem.* 266: 11192–11198.

Ascher, P., W. A. Large, and H. P. Rang. 1979. Studies on the mechanism of action of acetylcholine antagonists on rat parasympathetic ganglion cells. *J. Physiol. (Lond.).* 295:139–170.

Bertrand, D., M. Ballivet, and D. Rungger. 1990. Activation and blocking of neuronal nicotinic acetylcholine receptor reconstituted in *Xenopus* oocytes. *Proc. Natl. Acad. Sci. U.S.A.* 87:1993–1997.

Boulter, J., J. Connolly, E. Deneris, D. Goldman, S. Heinemann, and J. Patrick. 1987. Functional expression of two neural nicotinic acetylcholine receptors from cDNA clones identifies a gene family. *Proc. Natl. Acad. Sci. U.S.A.* 84:7763–7767.

Changeux, J.-P., A. Devillers-Thiery, J.-L. Galzi, and D. Bertrand. 1992. The functional architecture of the acetylcholine nicotinic receptor explored by affinity labeling and site- directed mutagenesis. *Q. Rev. Biophys.* 25:395–432.

Charnet, P., C. Labarca, R. J. Leonard, N. J. Vogelaar, L. Czyzyk, A. Gouin, N. Davidson, and H. A. Lester. 1990. An open-channel blocker interacts with adjacent turns of α-helices in the nicotinic acetylcholine receptor. *Neuron.* 2:87–95.

Conroy, W. G., and D. K. Berg. 1995. Neurons can maintain multiple classes of nicotinic acetylcholine receptors distinguished by different subunit compositions. *J. Biol. Chem.* 270:4424–4431.

Cooper, E., S. Couturier, and M. Ballivet. 1991. Pentameric structure and subunit stoichiometry of a neuronal nicotinic acetylcholine receptor. *Nature.* 350:235–238.

DiPaola, M., P. Kao, and A. Karlin. 1990. Mapping the alpha subunit site photolabeled by the noncompetitive inhibitor [^{3}H]-quinacrine azide in the active state of the nicotinic acetylcholine receptor. *J. Biol. Chem.* 265:11017–11029.

Francis, M. M., and R. L. Papke. 1996. Muscle-type nicotinic acetylcholine receptor delta subunit determines sensitivity to noncompetitive inhibitors while gamma subunit regulates divalent permeability. *Neuropharmacology.* 35:1547–1556.

Gerzanich, V., A. Kuryatov, R. Anand, and J. Lindstrom. 1997. "Orphan" α6 nicotinic AChR subunit can form a functional heteromeric acetylcholine receptor. *Mol. Pharmacol.* 51:320–327.

Giraudat, J., M. Dennis, T. Heidmann, J. Y. Chang, and J.-P. Changeux. 1986. Structure of the high affinity binding site for noncompetitive blockers of the acetylcholine receptor: serine-262 of the delta subunit is labeled by [^{3}H]chlorpromazine. *Proc. Natl. Acad. Sci. U.S.A.* 83: 2719–2723.

Giraudat, J., M. Dennis, T. Heidmann, P.-Y. Haumont, F. Lederer, and J.-P. Changeux. 1987. Structure of the high affinity binding site for the noncompetitive blockers of the acetylcholine receptor. [^{3}H]-Chlorpromazine labels homologous residues in the β and δ chains. *Biochemistry.* 26:2410–2418.

Glossmann, H., S. Hering, A. Savchenko, W. Berger, K. Friedrich, M. L. Garcia, M. A. Goetz, J. M. Liesch, D. L. Zink, and G. J. Kaczorowski. 1993. A light stabilizer (Tinuvin 770) that elutes from polypropylene plastic tubes is a potent L-type Ca^{2+}-channel blocker. *Proc. Natl. Acad. Sci. U.S.A.* 90:9523–9527.

Holtzman, E., D. Wise, J. Wall, and A. Karlin. 1981. Electron microscopy of complexes of isolated acetylcholine receptor biotinyl-toxin and avidin. *Proc. Natl. Acad. Sci. U.S.A.* 79:310–314.

Horton, R. M., H. D. Hunt, S. N. Ho, J. K. Pullen, and L. R. Pease. 1989. Engineering hybrid genes without the use of restriction enzymes: gene splicing by overlap extension. *Gene.* 77:61–68.

Ifune, C. K., and J. H. Steinbach. 1992. Inward rectification of acetylcholine-elicited currents in rat phaeochromocytoma cells. *J. Physiol. (Lond.).* 457:143–165.

Imoto, K., C. Busch, B. Sakmann, M. Mishina, T. Konno, J. Nakai, H. Bujo, Y. Mori, K. Fukuda, and S. Numa. 1988. Rings of negatively charged amino acids determine the acetylcholine receptors channel conductance. *Nature.* 335:645–648.

Karlin, A., and M. H. Akabas. 1995. Toward a structural basis for the function of nicotinic acetylcholine receptor and their cousins. *Neuron.* 15:1231–1244.

Karlin, A., E. Holtzman, N. Yodh, P. Lobel, J. Wall, and J. Hainfeld. 1983. The arrangement of the subunits of the acetylcholine receptor of *Torpedo californica. J. Biol. Chem.* 258:6678–6681.

Kearney, P. C., H. Zhang, W. Zhong, D. A. Dougherty, and H. A. Lester. 1996. Determinants of nicotinic receptor gating in natural and unnatural side chain structures at the M2 9′ position. *Neuron.* 17:1221–1229.

Lee, G. E., W. R. Wragg, S. J. Corne, N. D. Edge, and H. W. Reading. 1958. 1:2:2:6:6-Pentamethylpiperidine: a new hypotensive drug. *Nature.* 181:1717–1719.

Leonard, R. J., C. G. Labarca, P. Charnet, N. Davidson, and H. A. Lester. 1988. Evidence that the M2 membrane-spanning region lines the ion channel pore of the nicotinic receptor. *Science.* 242:1578–1581.

Luetje, C. W., and J. Patrick. 1991. Both α- and β-subunits contribute to the agonist sensitivity of neuronal nicotinic acetylcholine receptors. *J. Neurosci.* 11:837–845.

Machold, J., C. Weise, Y. Utkin, V. Tsetlin, and F. Hucho. 1995. The handedness of the subunit arrangement of the nicotinic acetylcholine receptor from *Torpedo californica. Eur. J. Biochem.* 234:427–430.

Miller, C. 1989. Genetic manipulation of ion channels: a new approach to structure and mechanism. *Neuron.* 2:1195–1205.

Neher, E., and J. H. Steinbach. 1978. Local anaesthetics transiently block current through single acetylcholine receptor channels. *J. Physiol. (Lond.).* 277:135–176.

Papke, R. L. 1993. The kinetic properties of neuronal nicotinic receptors: genetic basis of functional diversity. *Prog. Neurobiol.* 41:509–531.

Papke, R. L., A. G. Craig, and S. F. Heinemann. 1994. Inhibition of nicotinic acetylcholine receptors by BTMPS, (Tinuvin 770), an additive to medical plastics. *J. Pharmacol. Exp. Ther.* 268:718–726.

Papke, R. L., and S. F. Heinemann. 1991. The role of the β4 subunit in determining the kinetic properties of rat neuronal nicotinic acetylcholine α3-receptor. *J. Physiol. (Lond.).* 440:95–112.

Papke, R. L., and R. E. Oswald. 1989. Mechanisms of noncompetitive inhibition of acetylcholine-induced single channel currents. *J. Gen. Physiol.* 93:785–811.

Pascual, J. M., and A. Karlin. 1997. Binding site for QX-314, a quaternary lidocaine derivative, in the channel of the acetylcholine receptor. *Biophys. J.* 72:A151.

Pedersen, S. E., S. D. Sharp, W. S. Liu, and J. B. Cohen. 1992. Structure of the noncompetitive antagonist-binding site of the *Torpedo* nicotinic acetylcholine receptor. [^{3}H]Meproadifen mustard reacts selectively with alpha-subunit Glu-262. *J. Biol. Chem.* 267:10489–10499.

Perrin, D. D. 1965. Dissociation Constants of Organic Bases in Aqueous Solution. Butterworths, London.

Sands, S. B., and M. E. Barish. 1992. Neuronal nicotinic acetylcholine receptor currents in phaeochromocytoma (PC12) cells: dual mechanisms of rectification. *J. Physiol. (Lond.).* 447:467- 487.

Sanger, F., S. Nicklen, and A. R. Coulson. 1977. DNA sequencing with chain-terminating inhibitors. *Proc. Natl. Acad. Sci. U.S.A.* 74: 5463–5467.

Sargent, P. B. 1993. The diversity of neuronal nicotinic acetylcholine receptors. *Annu. Rev. Neurosci.* 16:403–443.

Spinks, A., and E. H. P. Young. 1958. Polyalkylpiperidines: a new series of ganglion-blocking agents. *Nature.* 181:1397–1398.

White, B. H., and J. B. Cohen. 1992. Agonist-induced changes in the structure of the acetylcholine receptor M2 regions revealed by photoincorporation of an uncharged nicotinic noncompetitive antagonist. *J. Biol. Chem.* 267:15770–15783.

Zhang, H., and A. Karlin. 1996. Acetylcholine receptor channel-lining residues in the M2 segment of the β-subunit. *Proc. Annu. Meeting Soc. Neurosci., 26th.* 110.1.

Zhorov, B. S., N. B. Brovtsyna, V. E. Gmiros, N. Y. Lukomskaya, S. Y. Serdyuk, N. N. Potapyeva, L. G. Magazanik, D. E. Kurenniy, and V. I. Skok. 1991. Dimensions of the ion channel in neuronal nicotinic acetylcholine receptor as estimated from conformation-activity relationships of open-channel blocking drugs. *J. Membr. Biol.* 121:119–132.